Mathematical and Computer Modelling 50 (2009) 959–974

Contents lists available at ScienceDirect

Mathematical and Computer Modelling

journal homepage: www.elsevier.com/locate/mcm

A mathematical model for the first-pass dynamics of antibiotics acting on the cardiovascular system

H.T. Banks [a,b,*], Kathleen Holm [a,b,c], Nathan C. Wanner [a,b,c], Ariel Cintrón-Arias [a,b], Grace M. Kepler [a,b], Jeffrey D. Wetherington [d]

[a] Center for Research in Scientific Computation (Box 8212), North Carolina State University, Raleigh, NC 27695, United States
[b] Center for Quantitative Sciences in Biomedicine (Box 8213), North Carolina State University, Raleigh, NC 27695, United States
[c] Biomathematics Program (Box 8203), North Carolina State University, Raleigh, NC 27695, United States
[d] GlaxoSmithKline, 1 Franklin Plaza, 1FP1375, P.O. Box 7929, Philadelphia, PA 19102, United States

ARTICLE INFO

Article history:
Received 14 January 2009
Accepted 12 February 2009

Keywords:
Compartmental model
Circulatory system
Drug delivery
Differential equations
Optimal dosing strategies
Sensitivity

ABSTRACT

We present a preliminary first-pass dynamic model for delivery of drug compounds to the lungs and heart. We use a compartmental mass-balance approach to develop a system of nonlinear differential equations for mass accumulated in the heart as a result of intravenous injection. We discuss sensitivity analysis as well as methodology for minimizing mass in the heart while maximizing mass delivered to the lungs on a first circulatory pass.

1. Introduction

Pharmaceutical companies make significant investment in drug design and development which often primarily entails experiments and clinical trials. Mathematical models for drug uptake and metabolism can, if properly used, be of substantial value in this development process. In this paper we focus first on the process of developing such a model. We then illustrate the use of associated computational methodologies including optimization (maximizing drug delivery to target organs while minimizing amounts at other sensitive sites) and sensitivity analysis (with respect to model parameters and initial conditions. In particular we investigate the potential for first-pass effects on the heart that can result from intravenous (i.v.) administration of medicines relative to that for orally administered medicines. The goal of such a model is to determine a strategy for i.v. infusion that will minimize the risk of cardiovascular adverse effects given the chemical properties of the drug. Such models would prove to be very valuable for example in guiding dose administration in the treatment of pneumonia as some anti-bacterial agents carry cardiovascular liabilities. Alternatively, it could guide dose administration for an anti-cancer medicine in the treatment of lung cancer. Orally administered drugs do not pose this risk to patients. Also, model predictions could guide the synthesis of drug candidates. Because the model contains parameters describing drug absorption and metabolism, model predictions could help identify candidate drugs with properties that maximize efficacy in the lung (i.e., kill bacteria, arrest cancer cells) and minimize the risk of cardiovascular side effects (i.e., tachycardia).

To illustrate the modeling process for drug delivery and metabolism, we consider a class of antibiotics for the treatment of pneumonia with the lungs as target organs for delivery. We assume that the drugs are suspected of producing heart damage

* Corresponding author at: Center for Research in Scientific Computation (Box 8212), North Carolina State University, Raleigh, NC 27695, United States.
E-mail address: htbanks@ncsu.edu (H.T. Banks).

0895-7177/$ – see front matter © 2009 Published by Elsevier Ltd
doi:10.1016/j.mcm.2009.02.007

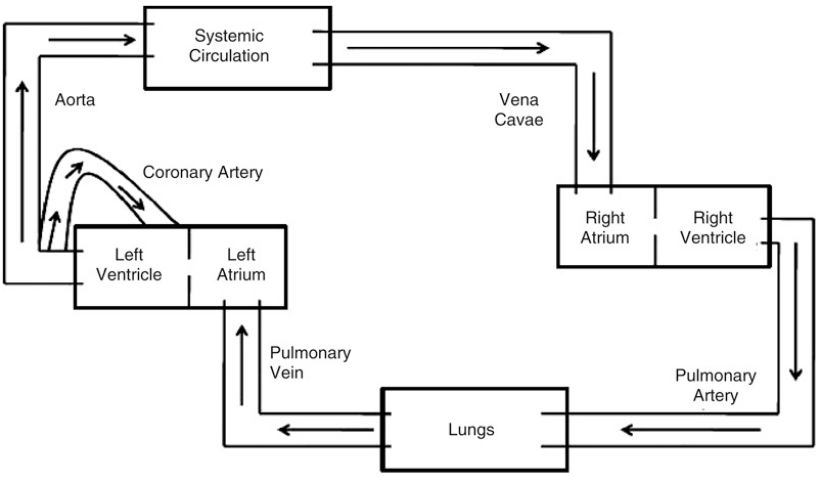

Fig. 1. Simplification of circulatory system.

Table 1
Time-dependent state variables.

State variable	Definition
M_P	Mass of drug in pulmonary artery
M_L	Mass of drug in blood supply to lung
M_T	Mass of drug in lung tissue
M_A	Mass of drug in ascending aorta
M_C	Mass of drug in blood supply to heart
M_H	Mass of drug in heart tissue

in organisms being treated. Pre-clinical trials in animals have shown that some antibiotics cause arrhythmias in the hearts of the animals when the drug is administered intravenously, and arrhythmias sometimes occur more frequently with a higher overall dose. This is a serious concern because these arrhythmias pose a heart attack risk. Arrhythmias do not occur when the compound is administered orally, but this may be explained by a lower overall dose.

Although the mechanism behind the drug-related arrhythmias is unknown, one hypothesis is that accumulation of the drug in the cardiac tissue, mostly from the first pass of the drug through the body, is one of the main factors. We develop a preliminary mathematical-pharmacokinetic model to analyze how the drug is distributed throughout the body for different dosage strategies. For a good overview of using differential equations to model components of the cardiovascular system see [1]. The main goal of the model used here is to predict, for a given dosage regimen, the accumulation of the drug in the cardiac and pulmonary tissue from its first pass through the organs. Because we are mostly concerned with the effects of the drug during its first pass through the system, we will not consider the effects of systemic circulation such as metabolism in the liver. With such models, one should be able to find an optimal dosing strategy that maximizes accumulation of the drug in the lungs, in order to treat pneumonia, while minimizing accumulation in the cardiac tissue.

In Section 2 we give details for a preliminary first-pass dynamic model for delivery of drug compounds to the lungs and heart. This is followed by simulation results reported in Section 3 along with a description of a computational methodology for choosing optimal injection strategies. A general methodology for sensitivity studies along with sample calculations are presented in Section 4.

2. Model description

A description of the model compartments, or state variables, along with the equations, parameters, and assumptions of the model will be given here. In compartmental modeling, a compartment can represent a physiological subdivision of a system throughout which the behavior of a substance is uniform [2], and an important part of the development of the model is how the compartments are chosen. A grossly simplified representation of the circulatory system can be seen in Fig. 1. After the drug is injected into a vein leading to the vena cavae, it passes through the right atrium, right ventricle, pulmonary artery, lungs, pulmonary vein, left atrium, left ventricle, aorta, coronary artery, and heart tissue.

As can be seen in Table 1, compartments were not created for all of these physiological parts. As the drug passes through the veins and arteries, it is assumed that no amount of the drug is lost, and all of the drug passes through. Inclusion of a vein or artery in the model ensures that the flow rate into the next compartment is represented correctly. Because we are mostly concerned with the flow rates of the drug into the heart and lung, compartments representing arteries preceding these two organs were included. While one could argue that including compartments for the pulmonary vein and right and left sides of the heart would make the model more accurate, additional compartments would require that more parameters be estimated.

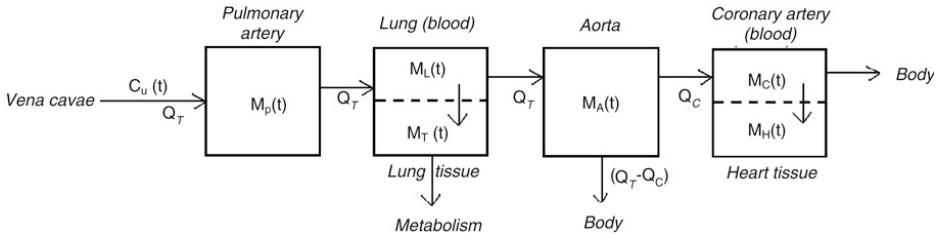

Fig. 2. Compartment model diagram.

In this initial model, we have attempted to balance the trade-off between the number of parameters contained in the model and accuracy of the mathematical representation of the physical system. Another reason the compartments were chosen as depicted is that scientists have the ability to take blood sample measurements at many of the physiological sites included as compartments in our model [3]. These measurements could be used in calibration and validation investigations of the model. A schematic of the model is given in Fig. 2, and mathematical descriptions of the rate at which the drug enters/exits the compartments in the model are presented in Eqs. (2.1)–(2.6). These equations were obtained (under assumptions described below) using mass-balance principles, and their initial conditions are given by (2.7).

$$\frac{dM_P}{dt} = C_U(t) - \frac{Q_T}{V_P}M_P(t) \tag{2.1}$$

$$\frac{dM_L}{dt} = \frac{Q_T}{V_P}M_P(t) - \left(a - \frac{aM_T(t)}{K_1 + M_T(t)}\right)M_L(t) - \frac{Q_T}{V_L}M_L(t) \tag{2.2}$$

$$\frac{dM_T}{dt} = \left(a - \frac{aM_T(t)}{K_1 + M_T(t)}\right)M_L(t) - \frac{bM_T(t)}{K_2 + M_T(t)}M_T(t) \tag{2.3}$$

$$\frac{dM_A}{dt} = \frac{Q_T}{V_L}M_L(t) - \frac{Q_T}{V_A}M_A(t) \tag{2.4}$$

$$\frac{dM_C}{dt} = \frac{Q_C}{V_A}M_A(t) - \left(c - \frac{cM_H(t)}{K_3 + M_H(t)}\right)M_C(t) - \frac{Q_C}{V_C}M_C(t) \tag{2.5}$$

$$\frac{dM_H}{dt} = \left(c - \frac{cM_H(t)}{K_3 + M_H(t)}\right)M_C(t) \tag{2.6}$$

$$M_P(t_0) = M_L(t_0) = M_T(t_0) = M_A(t_0) = M_C(t_0) = M_H(t_0) = 0. \tag{2.7}$$

The parameter $C_U(t)$ in Eq. (2.1) represents the rate at which the drug is injected at time t, and two different mathematical descriptions of the time-dependent parameter $C_U(t)$ for the case of constant injection rate are given in expressions (2.8) and (2.9):

$$C_U(t) = \begin{cases} fd & \text{if } 0 \le t \le \tau \\ 0 & \text{if } t > \tau, \end{cases} \tag{2.8}$$

$$C_U(t) = \begin{cases} f\dfrac{D}{T} & \text{if } 0 \le t \le T \\ 0 & \text{if } t > T. \end{cases} \tag{2.9}$$

In expression (2.8), d represents the dose rate, τ represents the dose delivery time, and f is the fraction of unbound drug in the blood plasma; in expression (2.9), D represents the total dose administered, and T is the dose delivery time. These two alternative descriptions of the injection rate allow for the investigation of different questions regarding dosing regimens. Fixing d and varying τ in (2.8) are analogous to injecting the drug at the same rate for different amounts of time, while fixing D and varying T in (2.9) represent applying the same total dose for different amounts of time.

Sheep are important animal models used for the study of drug kinetics and blood flow, and their body weight and size are similar to that of humans [4]. The values for the parameters in Table 2 represent the circulatory and cardiovascular systems of sheep, and values for many of the parameters were obtained from [3]. (We remark that the specific values obtained from [3] may not be appropriate for use in our first-pass model, but can be used to produce simulations illustrating the ideas and methodology presented in this paper.) Of these parameters, only Q_T and Q_C were measured directly in efforts reported in [3]; values for V_P, V_L, and V_C were estimated by fitting a model to data under conditions different from those in our investigations here. A value for the volume of the ascending aorta in sheep could not be found; however, a value was found for humans [5]. Using the human ascending aorta volume (.082 L) and a value of 5.0 L/min for the total cardiac output for humans [6], we obtained the sheep volume by assuming the ratio of ascending aorta volume to total cardiac output is equal between the two

Table 2
Parameter values.

Parameter	Definition and origin	Baseline value	Unit	Source
Q_T	Cardiac output (flow rate) (Bio)	5.6	L/min	[3]
V_P	Effective pulmonary mixing volume (Bio)	0.255	L	[3]
V_L	Volume of the lung (Bio)	1.06	L	[3]
a	Maximum rate for absorption into lung tissue (Chem)	1	$(\text{min})^{-1}$	Assumed
K_1	Shape parameter for absorption into lung (Chem)	1	mg	Assumed
b	Maximum rate for metabolism in lung (Chem)	0.10	$(\text{min})^{-1}$	Assumed
K_2	Shape parameter for metabolism in lung (Chem)	1	mg	Assumed
V_A	Volume of the ascending aorta (Bio)	0.10	L	Derived from [5]
Q_C	Flow rate through coronary artery (Bio)	0.122	L/min	[3]
V_C	Volume of the coronary artery (Bio)	0.45	L	[3]
c	Maximum rate for absorption into heart tissue (Chem)	1	$(\text{min})^{-1}$	Assumed
K_3	Shape parameter for absorption into heart tissue (Chem)	1	mg	Assumed
f	Fraction of unbound drug in blood plasma (Chem)	1	unitless	Assumed
d	Dose rate for equation (2.8) (Dose)	60	mg/min	Assumed
τ	Dose delivery time for (2.8) (Dose)	0.50	min	Assumed
D	Total dose administered for (2.9) (Dose)	100	mg	Assumed
T	Dose delivery time for (2.9) (Dose)	0.50	min	Assumed

species and then rounded this value to the first significant digit. The parameters that are adjustable and will be interesting in attempts made to examine different dosing strategies include d, τ, D, and T. In Table 2 the parameters are denoted (Bio), (Chem), or (Dose) depending on whether their origin is biological (depending on the organism receiving the drug), chemical (depending on the properties of the drug) or dose related (depending on dosing strategy).

When building a mathematical model, it is important to clearly state all of the assumptions that are made, and a summary of those underlying this model is presented next.

(i) In the model represented by Eqs. (2.1)–(2.7), each of the compartments have a constant volume and are well-mixed.

(ii) After injection, typically into a vein leading to the vena cavae, the drug travels from the injection site to the pulmonary artery, which is the input to the lung, an organ of interest in this work. Enroute to the lung, the distribution of the drug is affected by dilution with other venous flow comprising the total cardiac output Q_T, dispersion, mixing, and plasma binding. Eq. (2.1) accounts for the effective rate of change of the mass of the drug prior to entering the lung. The $C_U(t)$ term represents the unmixed rate of injection of the drug. The term V_P represents an effective mixing volume that accounts for the dispersion and mixing of the drug enroute to the lung [7]. The term $\frac{Q_T}{V_P}$ in Eq. (2.1) represents the rate of flow out of the pulmonary artery. An important assumption being made in both representations of $C_U(t)$ (Eqs. (2.8) and (2.9)) is that in the absence of plasma binding (i.e., the fraction of unbound drug in the plasma is 1), the drug enters the pulmonary artery at the same rate it was injected. It is also assumed that the drug injection does not affect blood flow; this assumption is valid if the volume of the solution containing the injected drug is small. With respect to injection of different doses, the current version of the model compares injecting different concentrations of the drug in a small fixed volume of solution (i.e., the total mass injected is allowed to vary but the volume of the solution containing the drug does not change). It is also assumed that neither the vena cavae nor the right side of the heart are affecting the rate at which the drug enters the pulmonary artery.

(iii) Similar to the manner in which the effects of the vena cavae and right side of the heart on the drug flow rate were ignored, it is assumed that the pulmonary vein and left side of the heart do not affect the flow of the drug.

(iv) The organ compartments corresponding to the heart and lung can each be modeled with two compartments. For each organ, there is a compartment representing the blood supply to the organ as well as a compartment for the organ tissue. When modeling organ compartments in physiology, it is common practice to use separate compartments for the blood and tissue parts [8], and this is the approach we have taken for the two organs in our system.

(v) Eq. (2.2) describes the flow into and out of the blood supply of the lung. The term $\frac{Q_T}{V_P}$ represents flow into the blood supply of the lung. The exchange between the M_P and M_L compartments is analogous to an exchange that occurs in a connection between two pipes, and we are assuming here that the flow out of the M_P compartment is equal to the flow into the M_L compartment. The outflow term in the M_L compartment contains the parameter V_L representing the volume of the lung, and similar inflow and outflow terms can be found in the M_A compartment.

(vi) Although the pulmonary artery, lung, and aortic arch receive the entire blood supply of the body, the coronary artery only receives a fraction of this supply which is represented by the parameter Q_C. The inflow and outflow terms in the M_C compartment do not involve the Q_T parameter but instead involve the parameter Q_C which is smaller than Q_T.

(vii) We are left with three nonlinear terms in the model to discuss:

$$a - \frac{aM_T(t)}{K_1 + M_T(t)}, \qquad \frac{bM_T(t)}{K_2 + M_T(t)}, \quad \text{and} \quad c - \frac{cM_H(t)}{K_3 + M_H(t)},$$

which represent absorption into the lung tissue, metabolism in the lung tissue, and absorption into the heart tissue, respectively. The parameters in these terms are heavily dependent upon the particular drug under investigation. The

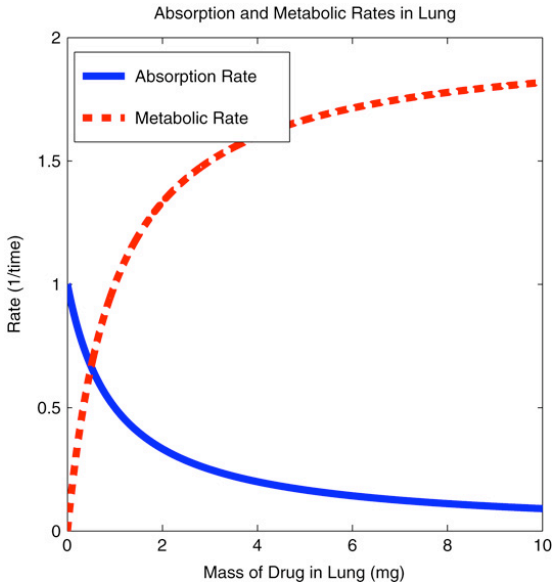

Fig. 3. Absorption and metabolic rates in lung as function of M_T for parameter values $a = 1$, $b = 2$, $K_1 = 1$, $K_2 = 1$.

first of these terms is found in equations (2.2) and (2.3) and represents the rate at which the drug is absorbed into the lung tissue from the blood supply to the lung. Here a is a parameter representing the maximum absorption rate into the lung with units of $(\text{time})^{-1}$, and K_1 dictates how fast the rate of absorption decreases as the mass of the drug in the lung tissue increases. In the second term, $\frac{bM_T(t)}{K_2+M_T(t)}$, b is a parameter that represents the maximum metabolic rate of the drug in the lungs, and K_2 determines how fast the metabolic rate saturates. It is known that enzyme-mediated binding and metabolism in the lungs are saturable processes ([9,7]), and these two terms are represented in Briggs–Haldane Michaelis-Menten form (see [10–13]). Plots of the absorption and metabolic rates as functions of M_T are presented in Fig. 3, and values chosen for the parameters are given in the plot. The curve for the absorption rate in the lung intersects the vertical axis at a and then approaches zero as M_T goes to infinity. The metabolic rate curve starts out at zero for $M_T = 0$ and then approaches b as M_T increases. When the absorption rate curve is greater than the metabolic rate curve, accumulation in the lung will occur; however, when the metabolic rate curve is greater, there will be a net loss of drug mass in the lung tissue. The term $(c - \frac{cM_H(t)}{K_3+M_H(t)})$ in equations (2.5) and (2.6) represents absorption of the drug into the heart tissue, and here the form was also chosen so that the absorption process is saturable.

(viii) While it is known that organs can serve as reservoirs that accumulate drug in their tissue and then release the drug later, this process was omitted in the current version of the model. Because our model is made to study the first-pass effects of the drug through the heart and lung organs, it is reasonable to ignore the release of tissue-bound drug mass.

3. Numerical results and optimization methodology

Typical model outputs $M_P(t), M_L(t), M_T(t), M_A(t), M_C(t)$, and $M_H(t)$ for the compartments are given in Fig. 4 for different values of D and T in expression (2.9). In particular, the graphs in Fig. 4 depict trajectories for drug concentrations in various model compartments in response to three different sets of dosing parameters D and T. The purpose of this section is to also illustrate the other types of computations that can be performed using our model. These computations can be used to explore questions that may be more difficult or more costly to answer experimentally. There are many goals that can be specified regarding the trajectory of the mass of the drug in the heart and lung. For instance, one may wish to maximize the ratio of peak mass or total mass of the drug that reaches the lung as compared to the heart. Here we will mathematically formulate the goal of, given a fixed dose, finding the best delivery time to maximize these ratios. Note that the total circulation time in humans is about 1 min [6]. Because our model was developed to analyze the first-pass distribution dynamics of a drug, it is only meaningful to use the model to examine dosage times where the dose will pass from the injection site through the coronary artery in less than one minute (assuming that total circulation time in humans and sheep is similar). It takes time for the drug to move between compartments, and so in order to be conservative, only injection times less than or equal to 30 s will be considered here.

Expressions (2.8) and (2.9) are only two possible mathematical representations of the drug injection, and they represent injecting the drug at a constant rate. We have freedom to choose the form for the time-dependent parameter $C_U(t)$, and other injection strategies are considered here to examine how the input function changes the output of the model. One additional form for the input can be seen in expression (3.1). In a clinical setting, this injection strategy represents constantly increasing the injection rate to a maximum at $t = T/2$, and then constantly decreasing the rate back down to zero from $t = T/2$ to

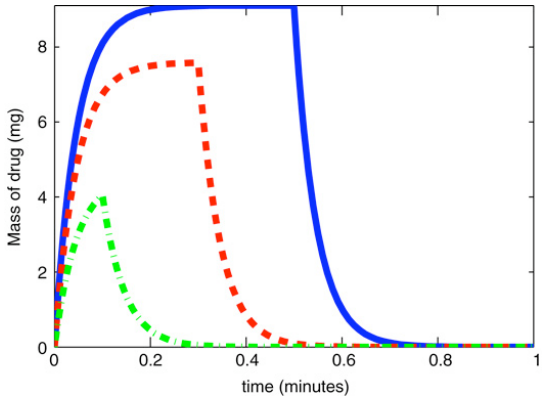

(a) Mass of drug in pulmonary artery vs. time.

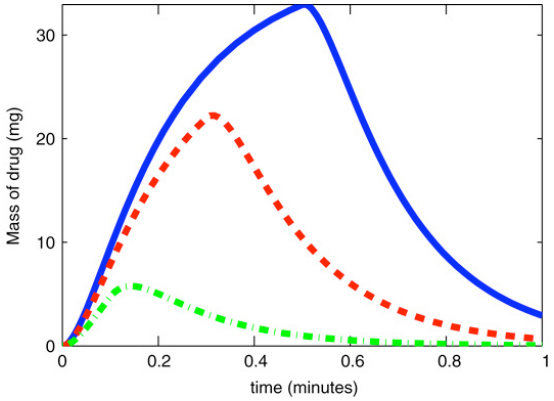

(b) Mass of drug in blood supply to lung vs. time.

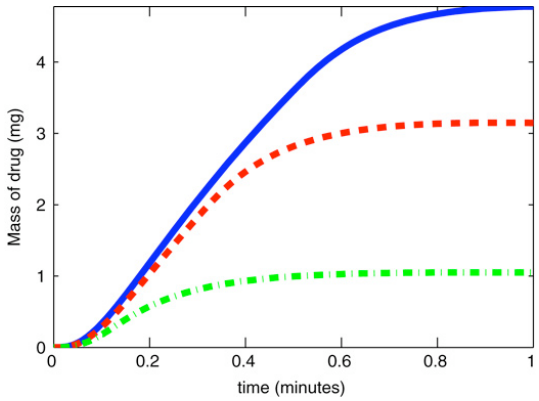

(c) Mass of drug in lung tissue vs. time.

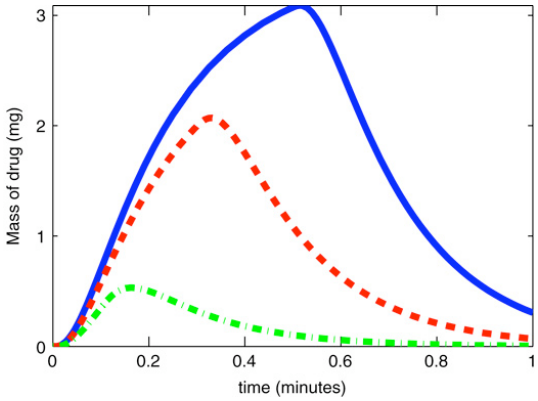

(d) Mass of drug in ascending aorta vs. time.

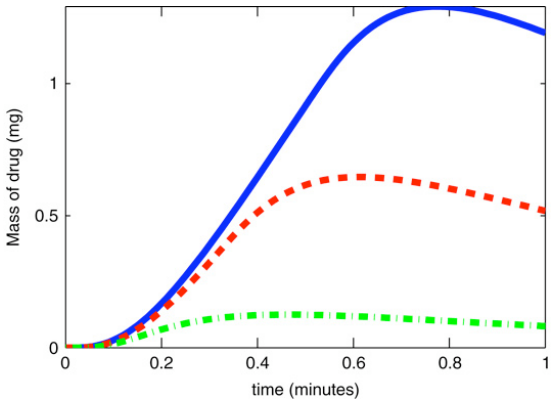

(e) Mass of drug in blood supply to heart vs. time.

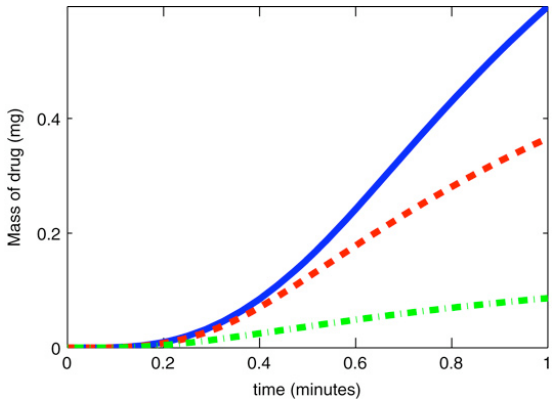

(f) Mass of drug in heart tissue vs. time.

Fig. 4. Model output for parameter values found in Table 2 with varying values of D and T: $D = 100$, $T = .5$ (solid line); $D = 50$, $T = .3$ (dashed line); $D = 10$, $T = .1$ (dot-dash line).

$t = T$. Geometrically, the expression represents an isosceles triangle, and the equation was derived using the formula for the area of a triangle and assuming the maximum height of the triangle occurs at $t = T/2$. A plot of this input function (along with the constant rate input function and several other considered input functions) can be seen in Fig. 5.

$$C_U(t) = \begin{cases} \dfrac{4f\frac{D}{T}t}{T} & \text{if } 0 \le t \le T/2 \\ \dfrac{-4f\frac{D}{T}t}{T} + 4\dfrac{D}{T} & \text{if } T/2 < t \le T \\ 0 & \text{if } T < t. \end{cases} \tag{3.1}$$

Another form for $C_U(t)$ is given by expression (3.2); note the addition of two new parameters—namely α, and β. This function was obtained by transforming a beta distribution (which is usually defined between zero and 1) to be defined for t

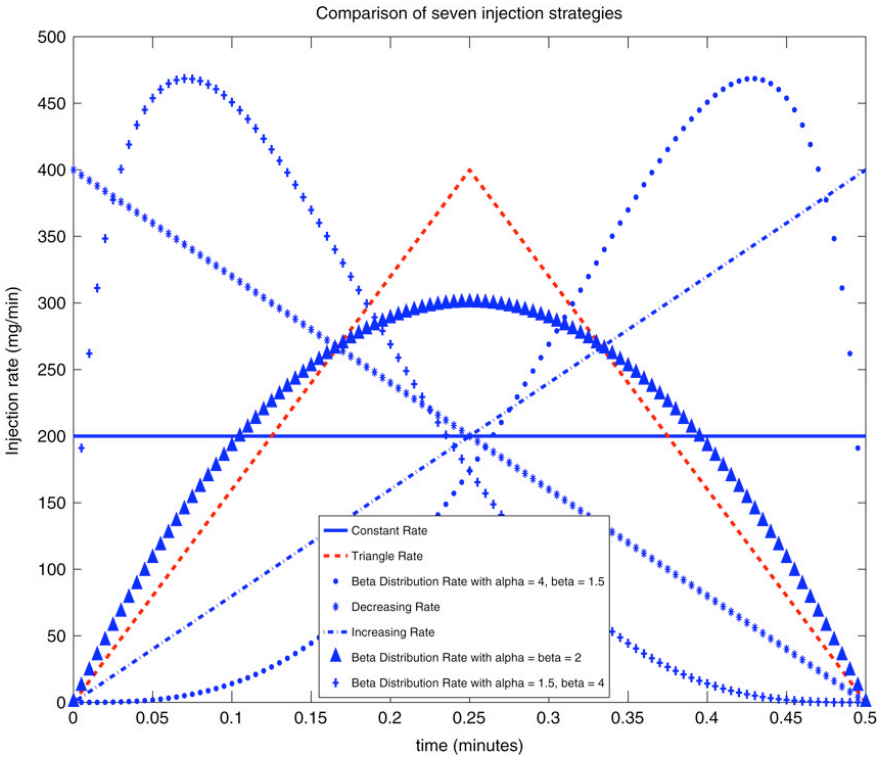

Fig. 5. Comparison of different injection strategies with $T = .5$ min and $D = 100$ mg.

between 0 and T and to have the area under the function be D. Using the transformed beta distribution for the input allows one to examine a large number of shapes for the input function by changing the shape parameters α and β. Visualizations of the transformed beta distribution input for a few different combinations of α and β are also given in Fig. 5. Mathematical expressions for two more injection strategies in Fig. 5 named the increasing and decreasing injection rate strategies were obtained similar to the manner in which the equation for the triangle injection rate strategy was obtained (equations for these input functions are not written explicitly here). A visualization of how the trajectories for the distribution of the drug in the heart and lung change for the different injection strategies with D fixed at 100 mg and T fixed at 0.5 min can be seen in Fig. 6.

$$C_U(t) = \begin{cases} f\dfrac{D}{T}\dfrac{\Gamma(\alpha+\beta)}{\Gamma(\alpha)\Gamma(\beta)}\dfrac{t^{\alpha-1}}{T}\left(1-\dfrac{t}{T}\right)^{\beta-1} & \text{if } 0 \le t \le T \\ 0 & \text{if } T < t. \end{cases} \tag{3.2}$$

Using well-defined mathematical descriptions of the goal one wishes to achieve with a dosage strategy, one can perform optimizations on cost functions to find the best strategy. Descriptions of some possible cost functionals are given in (3.3)–(3.6). When attempting to perform these optimizations, it became clear that the parameter values given in Table 2 cannot be correct. The important dynamics of the distribution of the drug should occur within the total circulation time as long as the injection time is sufficiently short, and this is not the case when using the parameters given in Table 2. To mitigate this difficulty and allow demonstration computations for the optimization ideas with the model, the parameter V_L (the volume of the lung) was changed to .25 L and the parameter V_C (the volume of the coronary artery) was changed to.01 L; the main purpose of these changes was to cause the drug to move through the system faster.

In (3.3) the objective is to find the dosage time between zero and 15 s that minimizes the ratio of peak drug mass in the heart to peak drug mass in the lung; this is equivalent to maximizing the ratio of peak mass in the lung to peak mass in the heart. Using the MATLAB optimization routine *fminsearch*() with an initial guess of .125 min, it was found that shorter injection times minimize the functional corresponding to (3.3). Indeed, as the tolerances of the optimization routine were made more stringent, the optimization routine returned shorter injection times. This suggests that to minimize the ratio of peak masses, the injection interval should be made as short as possible. This is confirmed in Fig. 7, where a plot of the ratio of peak masses for different injection strategies is shown. In the plot, one can see that regardless of the injection strategy, the ratio of peak drug mass in the lung to peak drug mass in the heart is maximized when the injection interval is short. However, notice that for longer injection times, some injection strategies perform better than others.

The functional in (3.4) corresponds to finding a dosage time between zero and 15 s that minimizes the ratio of total drug load in the heart to total drug load in the lung over one minute (or equivalently, maximizing the inverse). Interestingly, completely different results from those above are obtained when using the functional (3.4). It was found that if the goal is to

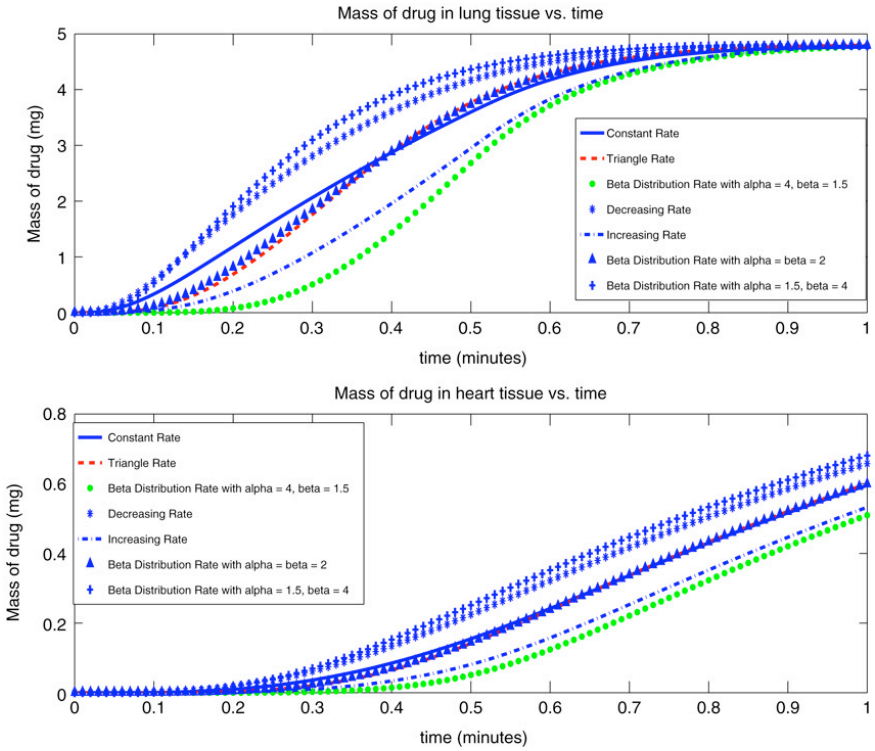

Fig. 6. Plots of M_T and M_H for seven different injection strategies shown in Fig. 5.

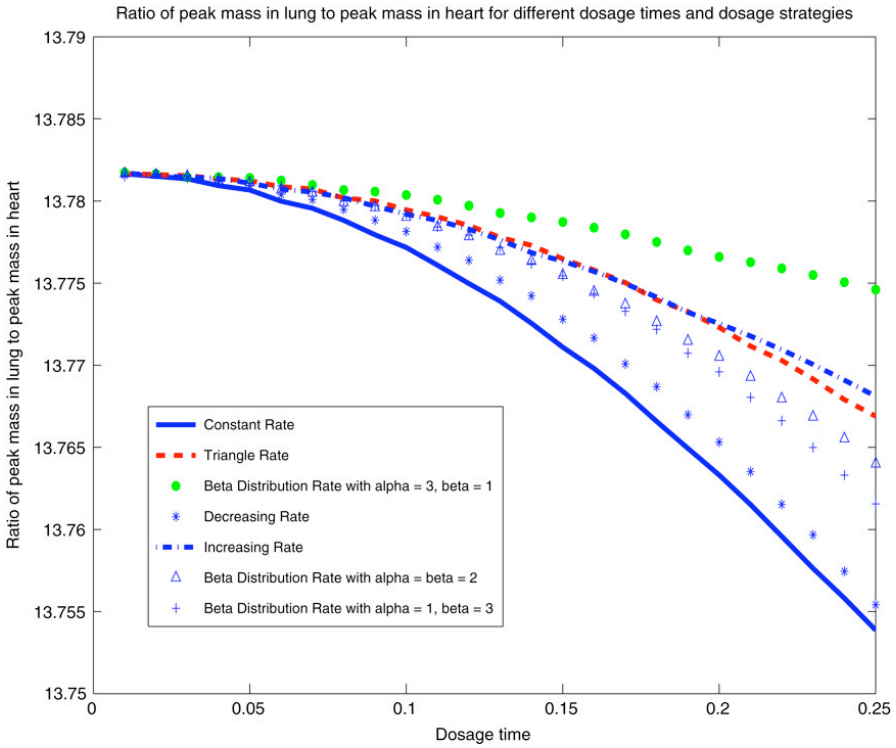

Fig. 7. Plot of the ratio of peak drug mass in the lung to peak drug mass in the heart for different dosing strategies and injection times. Injection times were sampled from .01 to .25 min with a step-size of .01.

maximize the total drug load in the lung to total drug load in the heart, longer injection times should be used. When applying the MATLAB optimization routine *fmincon*() to minimize the ratio of total drug load in the heart to total drug load in the lung with an initial guess of .125 min, the optimization routine returns the constraint on the injection time. For example, when the injection time is constrained to be less than .25 min as in (3.4), the optimal time returned by the optimization routine is

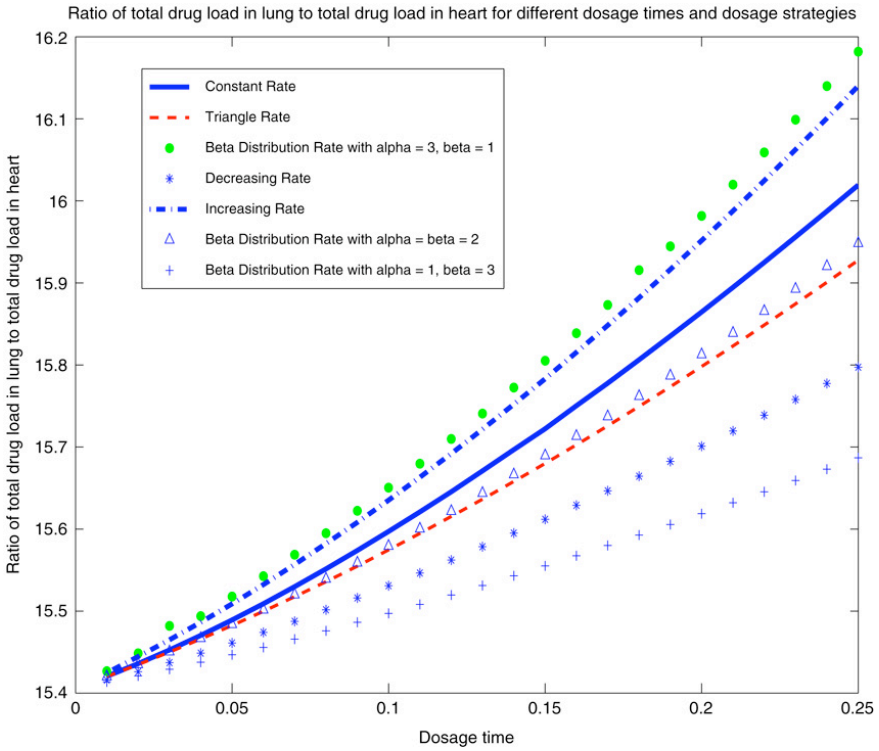

Fig. 8. Plot of the ratio of total drug load in the lung to total drug load in the heart over one minute for different dosing strategies and injection times. Injection times were sampled from .01 to .25 min with a step-size of .01.

.25 min. This suggests that to maximize the ratio of total drug loads in the lung and heart, longer injection intervals do better. Fig. 8 shows how the total drug load ratio increases as the injection time increases regardless of the injection strategy. Notice again that the differences between the injection strategies are minimal for small injection times, but the differences grow as the injection time increases. The differences between the results obtained when using the two different cost functionals illustrate the importance of clearly defining the goal of the injection for the distribution of the drug throughout the body.

$$\min_{0<T\leq.25}\left[\frac{\max_t(M_H(t;T))}{\max_t(M_T(t;T))}\right], \tag{3.3}$$

$$\min_{0<T\leq.25}\left[\frac{\int_0^1 M_H(t;T)\mathrm{d}t}{\int_0^1 M_T(t;T)\mathrm{d}t}\right]. \tag{3.4}$$

Optimizations performed in (3.5) and (3.6) are two more examples of the types of investigations that can be considered when searching for optimal dosing strategies and further illustrate the importance of clearly stating the goal regarding distribution of the drug during treatment. The cost functional in (3.5) is similar to that in (3.3) in that it corresponds to maximizing the peak mass of the drug in the lung to that in the heart; however, instead of searching for an optimal dosage time, T is constrained to be .25, and the objective is to find optimal shape parameters α and β. An analogous relationship exists between the cost functionals in (3.4) and (3.6)— both represent maximizing the total drug load in the lung as compared to the heart over the first pass of the drug through the body, but in (3.6) one optimizes the shape of the beta distribution input function for a fixed dosage time. Here the cost functionals do not involve the effects of changing the dose or the dosage time; they only examine changing the shape of the input function. When performing the optimizations in (3.5) and (3.6), α and β are constrained to be greater than or equal to 1, because these values give the input function a unimodal shape for the optimizations

$$\min_{\alpha,\beta\geq1}\left[\frac{\max_t(M_H(t;T=.25,\alpha,\beta))}{\max_t(M_T(t;T=.25,\alpha,\beta))}\right], \tag{3.5}$$

$$\min_{\alpha,\beta\geq1}\left[\frac{\int_0^1 M_H(t;T=.25,\alpha,\beta)\mathrm{d}t}{\int_0^1 M_T(t;T=.25,\alpha,\beta)\mathrm{d}t}\right]. \tag{3.6}$$

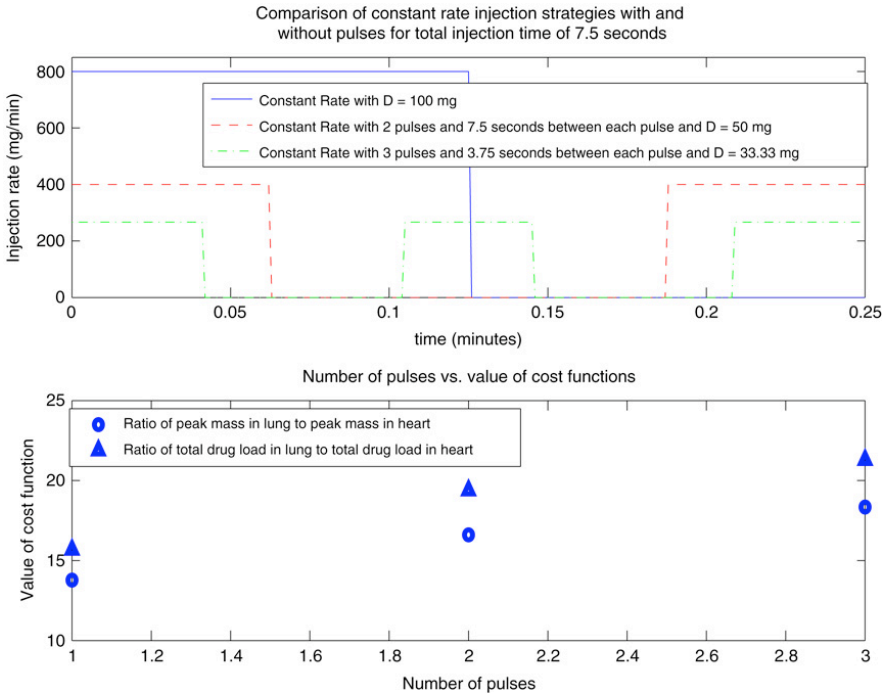

Fig. 9. Plot of constant rate injection strategy with different number of pulses and value of two ratios (peak mass of drug in lung to peak mass of drug in heart and total drug load in lung to total drug load in heart) as a function of the number of pulses.

Although different results were obtained for optimal dosage times depending on which cost function was being used, the optimal values for the shape parameters α and β seem to be the same regardless of which ratio is being considered. Optimizations performed on (3.5) and (3.6) revealed that α, β combinations with β equal to one and α greater than one perform best. One can see in Fig. 7 that when considering the ratio of peak masses, the beta distribution injection strategy with $\alpha = 3$ and $\beta = 1$ performs better than the others shown. Also, when considering the ratio of total drug loads in the heart and lung, the same values of α and β perform well. A plot of the beta distribution rate with these values of α and β is not shown here, but the input function with these parameters is uniform increasing and convex over the injection interval.

Note that in a clinical setting, it may be difficult or impossible to obtain some of these more complicated shapes for the injection input. However, this methodology was developed so that it may be applied when longer dosage intervals can be considered for a multiple-pass model. It should be emphasized that these results are sensitive to the parameters being used and may change for different parameter values. To obtain realistic predictions, precise parameter values are needed.

The last injection rate strategy examined in this section corresponds to a clinician administering different total amounts of the drug in a series of pulses—i.e., administering the drug at a constant rate, stopping the administration, re-administering the drug at a constant rate and so forth for a given number of times. A plot of this injection strategy can be seen in the top of Fig. 9 for 1 pulse and a total dose of 100 mg, 2 pulses (25 mg per pulse) and total dose of 50 mg, and 3 pulses (11.11 mg per pulse) and a total dose of 33.33 mg. These different dosing strategies permit consideration of the effects of administering a dose at a constant rate versus administering half that dose in two equal pulses versus administering 1/3 the original dose in three equal pulses without changing the total time that the dose is being injected. In the lower graph of Fig. 9 is a plot of the two different ratios we wish to maximize (peak mass and total load of the drug in the lung as compared to the heart) as a function of the number of pulses. While these simulations suggest that one can force more of a drug to reach the lung relative to the amount that reaches the heart by administering the drug in a series of pulses, better estimates for the parameters in the model are needed before these predictions can be taken seriously. Interestingly, this type of dosing strategy has been investigated by experimentalists, and Seltzer et al., found that they were able to obtain similar therapeutic effects when administering a drug in a bolus or by a series of pulses [14]. Trajectories of the distribution of the drug in the lung and heart over time for different numbers of pulses are plotted in Fig. 10. Observe that as the number of pulses increases, the trajectories for both the heart and lung tissue decrease; however, what is important is that the trajectories for the drug in the heart decrease faster causing the two ratios to increase as the number of pulses increases.

4. Sensitivity analysis

Sensitivity analysis is an important part of model analysis and validation. Sensitivity functions explicitly show the relationship between the parameters and the state variables. If model solutions are very sensitive to a particular parameter, one would want to have a reliable estimate for that parameter, as variations in the value of that parameter will affect the

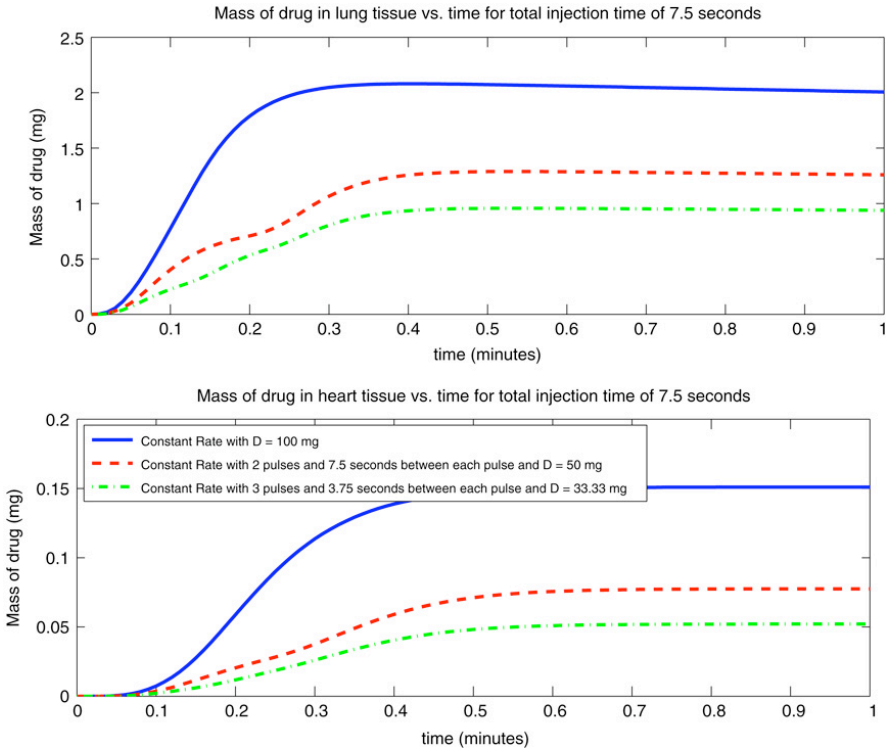

Fig. 10. M_T and M_H for constant rate injection strategy with several different pulsing strategies.

dynamics of solutions. Sensitivity functions are functions of time that describe how a state variable changes with respect to changes in a parameter. To define these sensitivity functions, we will re-state our model in vector notation.

We may define the p-vector of parameters by

$$\theta = (Q_T, V_P, V_L, a, K_1, b, K_2, V_A, Q_C, V_C, c, K_3, d), \tag{4.1}$$

and the n-vector state variable, for a given parameter vector θ and time t, as

$$x(t;\theta) = \begin{bmatrix} M_P(t;\theta) \\ M_L(t;\theta) \\ M_T(t;\theta) \\ M_A(t;\theta) \\ M_C(t;\theta) \\ M_H(t;\theta) \end{bmatrix}, \tag{4.2}$$

which allows us to write (2.1)–(2.6) in the compact form as

$$\frac{dx}{dt} = g(x(t;\theta);\theta), \tag{4.3}$$

where the vector function g is defined by the right side of (2.1)–(2.6). This form of the equations will be used in the sensitivity analysis.

The sensitivities of the state variables $(M_P, M_L, M_T, M_A, M_C, M_H)$ to the parameters $\theta = (Q_T, V_P, V_L, a, K_1, b, K_2, V_A, Q_C, V_C, c, K_3, d)$ were calculated. Our sensitivity analysis is described below, using a derivation obtained from [15].

Differentiating with respect to θ on both sides of (4.3), one obtains

$$\frac{\partial}{\partial\theta}\frac{dx}{dt} = \frac{\partial}{\partial\theta} g(x(t;\theta);\theta), \tag{4.4}$$

which implies that the $n \times p$ matrix $y = \partial x/\partial\theta$ satisfies

$$\frac{d}{dt}\frac{\partial x}{\partial\theta} = \frac{\partial g}{\partial x}\frac{\partial x}{\partial\theta} + \frac{\partial g}{\partial\theta}, \tag{4.5}$$

or equivalently,

$$\frac{dy}{dt} = \frac{\partial g}{\partial x} y + \frac{\partial g}{\partial\theta}. \tag{4.6}$$

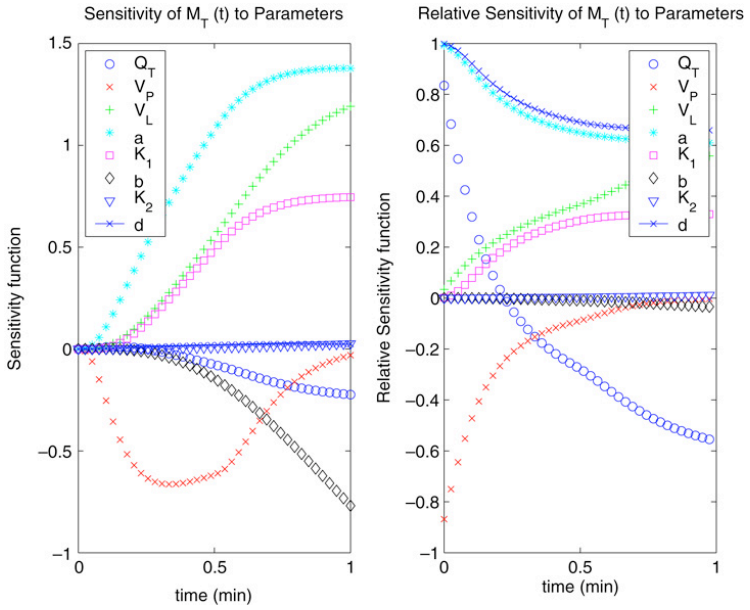

Fig. 11. Sensitivity and relative sensitivity functions for $M_T(t;\theta)$ to all parameters.

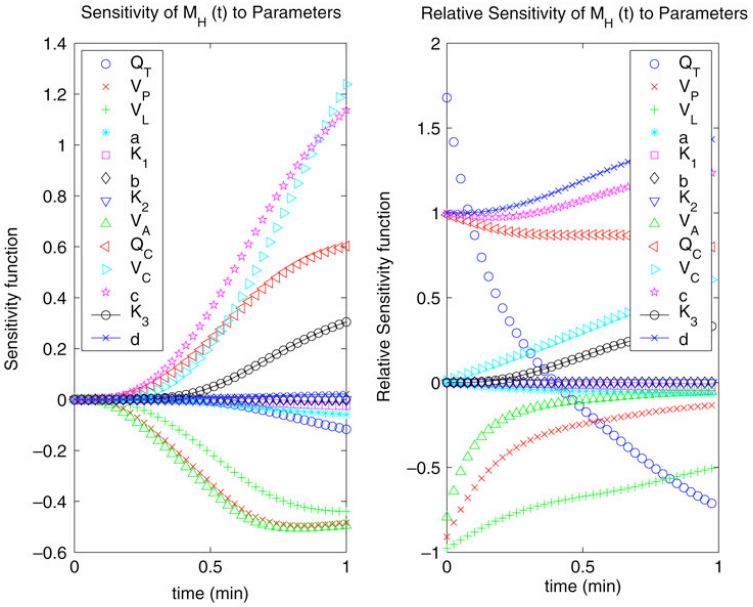

Fig. 12. Sensitivity and relative sensitivity functions for $M_H(t;\theta)$ to all parameters.

Numerical solutions of the sensitivity functions $y = (y_{ij}) = (\partial x_i/\partial\theta_j)$ are calculated by solving (4.3) and (4.6) simultaneously using $\theta = \tilde{\theta}$, where $\tilde{\theta}$ denotes a given value for the parameter. In our sensitivity analysis we used the parameter estimates listed in Table 2 for $\tilde{\theta}$. We note that in order to compute the sensitivity functions the model solutions are required to be continuous and differentiable with respect to the parameters. Because the equation for $C_U(t)$ was defined as in (2.8), a step function, we were not able to calculate the sensitivity to the dose time τ. However, with a reformulation of $C_U(t)$ as a smooth function of τ, one would be able to obtain sensitivity functions with respect to τ. We have 13 parameters and 6 state variables, hence computing the sensitivity function involves solving 78 first order differential equations (4.6). We can numerically solve this system of sensitivities simultaneously with the solutions of our model.

Relative sensitivities can be found using solutions $x(t;\theta)$, $\partial x(t;\theta)/\partial\theta$ and parameter estimate $\theta = \hat{\theta}$, by defining

$$rs_{ij} = \frac{\hat{\theta}_j}{x_i(t;\hat{\theta})}\frac{\partial x_i(t;\hat{\theta})}{\partial\theta_j}, \quad \text{for } i = 1,\ldots,n, j = 1,\ldots,p. \tag{4.7}$$

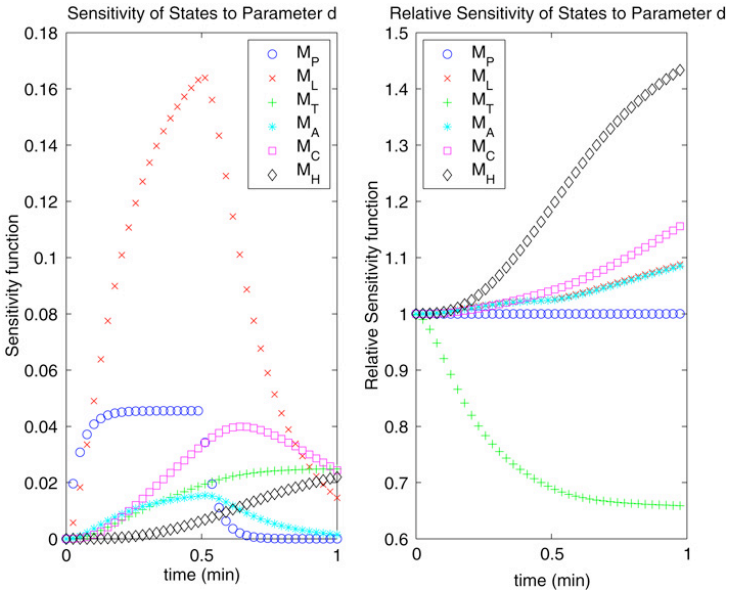

Fig. 13. Sensitivity and relative sensitivity functions for all states to parameter d.

4.1. Sensitivity results

Figs. 11–13 display some of the sensitivity and relative sensitivity solutions we obtained. The sensitivity functions look very different from the relative sensitivity functions. The sensitivity functions show the sensitivity of the state variables to the parameters which include the effect of the magnitude of the parameter estimates we used. However, the relative sensitivity functions are sensitivities scaled to account for the magnitude of the solutions and parameter estimates. These sensitivity functions change with time, indicating that a state variable may be sensitive to different sets of parameters depending on the time it is examined. This is important because if one is interested in the peak of the state solution, one could investigate to determine the parameters to which the model solutions are most sensitive at the time corresponding to the peak, before the peak, and after the peak. Note that if a sensitivity function for a state variable to a particular parameter was zero for all time, it was not plotted.

The sign of the sensitivity values corresponds to different effect variations in the parameter will have on the state variables. If the sensitivity function is positive in some time interval, increasing variations in that parameter, in that time interval, will cause the state variable to increase, depending on the magnitude of the sensitivity. Similarly, a negative sensitivity value implies that increasing variations in the parameter will cause the state variable to decrease. If the sensitivity function is zero for some time, the state variable is insensitive to that parameter. For example, in Fig. 11 (left) we can see that the sensitivity functions for $M_T(t;\theta)$ are strictly positive over the time span for parameters a, V_L, and K_1, and strictly negative for V_P, b, and Q_T. Upon close examination, we find that the sensitivity functions for $M_T(t;\theta)$ are close to zero but strictly positive for K_2 and d.

Figs. 11 and 12 offer a different perspective of our sensitivity analysis results from the results presented in Fig. 13. Figs. 11 and 12 depict the sensitivity functions for the state variables, $M_T(t,\theta)$ and $M_H(t,\theta)$, respectively, to all the parameters. Alternatively, Fig. 13 shows the sensitivities of all the state variables to only one parameter, d. These representations contain the same information, just organized differently. The representation of our sensitivity results in Fig. 13 is interesting since d is the dose rate, which is a parameter we have freedom to choose as input into our model. We may want to investigate how the variations in d will affect our model solutions over different time intervals. This relates to the analysis of different dosing strategies. For simplicity, we are only considering the constant rate dosing strategy in this sensitivity analysis. From Figs. 11–13 we conclude that sensitivity functions contain a lot of information that can be represented in different ways to offer different perspectives in a modeling effort.

At any fixed time, sensitivity functions can be ranked by the parameters to which given state variables are most sensitive. This is essentially what can be seen in Figs. 12 and 13. However it is useful to organize this information more concisely in a table. Because the relative sensitivity functions were solved for using a numerical differential equation solver, they are each discretized functions of time:

$$\vec{f} = (f(t_0), \ldots, f(t_N)) \in \ell_2^{N+1},$$

where $t_0, t_1, \ldots, t_N$ correspond to grid points for the numerical solution of the underlying differential equations (4.3) and (4.6). In order to rank the relative sensitivities of each state variable to all the parameters, we took the ℓ_2-norm of each relative sensitivity function where the ℓ_2-norm is defined as $|\vec{f}|_{\ell_2} = \left(\sum_{i=0}^{N} |f(t_i)|^2\right)^{\frac{1}{2}}$. The results of these relative sensitivity rankings can be found in Tables 3 and 4.

Table 3
The ℓ_2-norms of relative sensitivities for $M_P(t;\theta), M_L(t;\theta), M_T(t;\theta)$.

θ	$\left\lvert \frac{\hat{\theta}}{M_P}\frac{\partial M_P}{\partial \theta}\right\rvert_{\ell_2}$	θ	$\left\lvert \frac{\hat{\theta}}{M_L}\frac{\partial M_L}{\partial \theta}\right\rvert_{\ell_2}$	θ	$\left\lvert \frac{\hat{\theta}}{M_T}\frac{\partial M_T}{\partial \theta}\right\rvert_{\ell_2}$
V_P	52.1480	Q_T	16.2970	d	7.5154
Q_T	52.1480	V_L	14.3883	a	7.1472
d	9.9500	d	10.2853	Q_T	3.9814
V_L	0	V_P	3.1689	V_L	3.7544
a	0	a	0.6400	V_P	2.8898
K_1	0	K_1	0.4221	K_1	2.6723
b	0	b	0.0083	b	0.1551
K_2	0	K_2	0.0033	K_2	0.0569
V_A	0	V_A	0	V_A	0
Q_C	0	Q_C	0	Q_C	0
V_C	0	V_C	0	V_C	0
c	0	c	0	c	0
K_3	0	K_3	0	K_3	0

Table 4
The ℓ_2-norms of relative sensitivities for $M_A(t;\theta), M_C(t;\theta), M_H(t;\theta)$.

θ	$\left\lvert \frac{\hat{\theta}}{M_A}\frac{\partial M_A}{\partial \theta}\right\rvert_{\ell_2}$	θ	$\left\lvert \frac{\hat{\theta}}{M_C}\frac{\partial M_C}{\partial \theta}\right\rvert_{\ell_2}$	θ	$\left\lvert \frac{\hat{\theta}}{M_H}\frac{\partial M_H}{\partial \theta}\right\rvert_{\ell_2}$
Q_T	16.5474	d	10.4767	d	11.9227
d	10.2690	Q_T	8.6003	c	10.8097
V_A	9.8154	Q_C	6.5839	Q_C	8.7471
V_L	8.5873	V_L	5.3337	V_L	7.0754
V_P	3.2778	V_C	5.1970	Q_T	6.2522
a	0.6189	V_P	3.1814	V_P	3.8885
K_1	0.4041	V_A	2.1467	V_C	3.4543
b	0.0077	c	0.8924	V_A	2.5388
K_2	0.0030	a	0.4575	K_3	1.8980
Q_C	0	K_3	0.2946	a	0.4709
V_C	0	K_1	0.2231	K_1	0.1637
c	0	b	0.0024	b	0.0009
K_3	0	K_2	0.0011	K_2	0.0005

From Table 3, we can see that the state variable corresponding to our first compartment, $M_P(t;\theta)$, is only sensitive (has a nonzero ℓ_2-norm) to the parameters that are found in (2.1)—the model equation derived from mass balance of that compartment. However, from Tables 3 and 4, the other state variables are sensitive to the parameters found in their compartmental model equation, and the parameters that appeared in model equations of compartments upstream. The ranking of these parameters does not seem to follow any pattern corresponding to the flow of our compartments.

Sensitivity analysis is very important for compartmental modeling because it clearly shows the dependence of our model solutions on the parameter estimates we used. This sensitivity analysis was for the constant rate dosing strategy defined in (2.8). For a different dosing strategy, new sensitivity functions could readily be calculated.

5. Discussion and future work

Observations of the dynamics of the first pass of a drug through the heart led to this model formulation. Compartments were defined, and model equations were obtained using mass balance. Using plausible sheep parameter values found in the literature, we made numerical simulations of our model solutions, and analyzed these solutions for various dosing strategies. We also examined the sensitivity of our solutions to the parameter estimates we used. The analysis presented here demonstrates the capabilities of our model, but there is much more work that could be done.

For the purposes of this paper, values for the parameters corresponding to absorption of the drug into the lung (a and K_1), absorption into the heart (c and K_3), and metabolism in the lung (b and K_2) were assigned arbitrary values. To obtain more realistic estimates for these parameters specific to a given antibiotic being developed by a pharmaceutical company, experiments need to be performed. Indicator-dilution studies [16] have been used to quantify uptake of drugs in the lung, and this method could be used to determine more realistic parameter values for absorption into the lung for the drug. More precise values for the other parameters in the model also need to be obtained; many of the parameter values were taken from [3] where the authors obtained these when fitting a model different from ours to data. To obtain more appropriate values for these parameters, the values should be estimated using true first-pass experimental data in an appropriate inverse problem formulation. In addition, it is known that the anatomy of the circulatory system has a lot of interpersonal variability [17]. It would be interesting to compare sensitivity analysis predictions with real data on how this variability affects the distribution dynamics of the drug. Most of the parameters in the model are specific to individuals, and clinicians already use knowledge of pharmacokinetic parameters along with the factors that alter them to design optimal dosage regimens [18]. Experimental data on the variability of the pharmacokinetic parameters along with

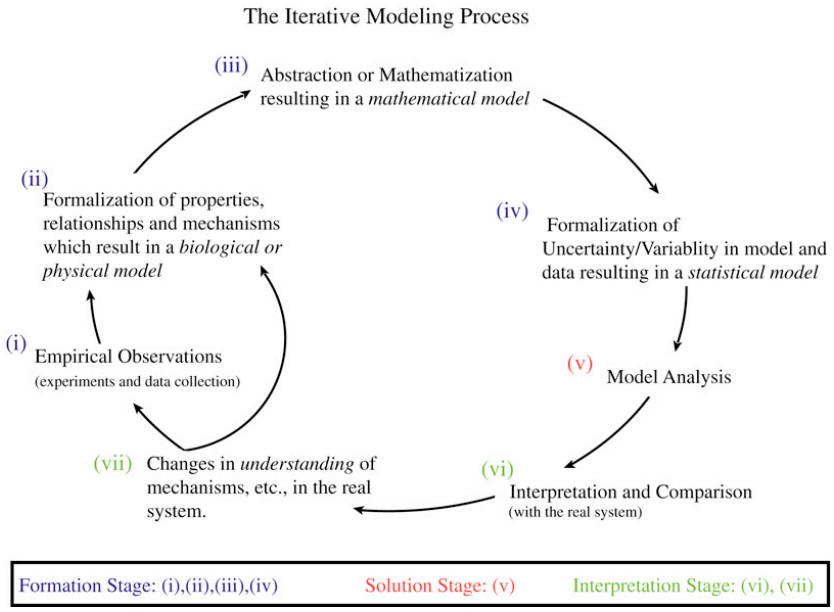

Fig. 14. Iterative modeling process.

the factors that affect these parameters specific to the drug being developed by a pharmaceutical company would help with making model predictions. Once reasonable model parameters are determined using experimental data for a given drug and organism, one could carry out meaningful simulations to compare drugs that are efficacious and safe; efficacious but with questionable safety; and efficacious but clearly unsafe. In addition, one could carry out simulations aimed at dosing strategies for attaining some minimum concentration in the lung tissue resulting in cure and some maximum concentration in heart tissue resulting in no side effects. That is, one could seek a threshold concentration in lungs such that all higher concentrations are efficacious; and a threshold concentration in the heart such that all lower concentrations are safe. This knowledge may better inform the drug development process. Finally, sensitivity calculations could be performed to determine mechanisms and areas of drug metabolism on which development should focus in future research.

It should be noted that the modeling process is iterative and should involve communication and collaboration with experimentalists. This iterative process is summarized in Fig. 14 and discussed in Chapter 1 of [2]. As the next step of the modeling process it would be helpful to obtain experimental data to validate our model (step (vi) from Fig. 14). As part of this process, we also need to carefully formulate the statistical model embedded in our mathematical model. Validation of the model using experimental data would allow for comparison of our model with the physiological system we attempted to describe. This most likely will lead to further refinement of our model, and another iteration of the modeling process. Through the communication that takes place between the mathematicians and the experimentalists in the iterative modeling process, the model will more accurately describe the physiological system, and can eventually be used for prediction.

Acknowledgements

We would like to thank Daniel Beavers (Baylor University), Abhishek Bhattacharya (University of Arizona), Matthew Causley (New Jersey Institute of Technology), and Juanjuan Chai (Indiana University) with whom this effort began as part of a summer research project [19] at the Industrial Mathematical and Statistical Modeling Workshop for Graduate Students sponsored by the Center for Research in Scientific Computation and the Statistical and Applied Mathematical Sciences Institute held at N.C. State University, July 21–29, 2008. Subsequent research was supported in part by the National Institute of Allergy and Infectious Disease under grant 9R01AI071915-05 and in part by the U.S. Air Force Office of Scientific Research under grant AFOSR-FA9550-08-1-0147. KH and NW were supported as CQSB Graduate Fellows during the course of their efforts.

References

[1] J.J. Batzel, F. Kappel, D. Schneditz, H.T. Tran, Cardiovascular and Respiratory Systems: Modeling, Analysis, and Control, SIAM, Philadelphia, 2007.
[2] H.T Banks, H.T. Tran, Mathematical and Experimental Modeling of Physical and Biological Processes, CRC Press, Boca Raton, 2009.
[3] R.N. Upton, A model of the first pass passage of drugs from i.v. injection site to the heart—parameter estimates for lignocaine in the sheep, British Journal of Anaethesia 77 (1996) 764–772.
[4] D. Adams, M. McKinley, The sheep, ANZCCART News 1995, 8: Insert.
[5] J.E.W. Beneken, B. DeWit, A physical approach to hemodynamic aspects of the human cardiovascular system, in: Physical Bases of Circulatory Transport; Regulation and Exchange; The Proceedings of a Conference Held in Sept. 1966, 1967, pp. 1–45.

[6] A. Noble, R. Johnson, A. Thomas, P. Bass, The Cardiovascular System, Churchill Livingstone, New York, 2005.
[7] R.N. Upton, D.J. Doolette, Kinetic aspects of drug disposition in the lungs, Clinical and Experimental Pharmacology and Physiology 26 (1999) 381–391.
[8] J.T. Ottesen, M.S. Olufsen, J.K. Larsen, Applied Mathematical Models in Human Physiology, SIAM, Washington DC, 2004.
[9] S.S. Cassidy, S.M. Scharf, Heart–Lung Interactions in Health and Disease, Marcel Dekker, Danbury, 1989.
[10] H.T. Banks, Modeling and Control in the Biomedical Sciences, in: Lecture Notes in Biomathematics, vol. 6, Springer-Verlag, Heidelberg, 1975.
[11] G.E. Briggs, J.B.S. Haldane, A note on the kinetics of enzyme action, Biochemistry 19 (1925) 338–339.
[12] L. Michaelis, M. Menten, Die Kinetik der Invertinwirkung, Biochemistry 49 (1913) 333–369.
[13] S.I. Rubinow, Introduction to Mathematical Biology, Wiley-Interscience, New York, 1975.
[14] J.L. Seltzer, J.I. Gerson, F.B. Allen, Comparison of the cardiovascular effects of bolus v. incremental administration of thiopentone, British Journal of Anaethesia 52 (1980) 527–530.
[15] P. Bai, H.T. Banks, S. Dediu, A.Y. Govan, M. Last, A.L. Lloyd, H.K. Nguyen, M.S. Olufsen, G. Rempala, B.D. Slenning, Stochastic and deterministic models for agricultural production networks, Mathematical Biosciences and Engineering 4 (3) (2007) 373–402.
[16] D.L. Roerig, K.J. Kotrly, C.A. Dawson, S.B. Ahlf, J.F. Gualtieri, J.P. Kampine, First-pass uptake of Verapamil, Diazepam, and Thiopental in the human lung, Anesthesia & Analgesia 69 (1989) 461–466.
[17] R. Uflacker, Atlas of Vascular Anatomy, Second ed., Lippincott Williams and Wilkins, Philadelphia, 2007.
[18] L.L. Brunton, J.S. Lazo, K.L. Parker, The Pharmacological Basis of Therapeutics, The McGraw-Hill Companies, New York, 2006.
[19] D. Beavers, A. Bhattacharya, M. Causley, J. Chai, K. Holm, N. Wanner, J. Wetherington, G.M. Kepler, H.T. Banks, A. Cintron-Arias, Cardiovascular events associated with oral and IV-administered antibacterial agents, in: Fourteenth Industrial Mathematical and Statistical Modeling Workshop for Graduate Students, Technical Report CRSC-TR08-21, NCSU, November, 2008.